Rotational spectra and structures of the Ar_2–$H^{35}Cl/^{37}Cl$ trimers

T. D. Klots, Carl Chuang, R. S. Ruoff, T. Emilsson, and H. S. Gutowsky
Noyes Chemical Laboratory, University of Illinois, Urbana, Illinois 61801

(Received 24 December 1986; accepted 21 January 1987)

Microwave rotational spectra have been observed for both Cl isotopes of the Ar_2–HCl trimer with the pulsed nozzle Fourier transform method using the Flygare Mark II spectrometer. The Cl nuclear quadrupole hyperfine structure was analyzed for each of the transitions and the coupling constants and line centers determined. Sixteen transitions were observed in the 2 to 15 GHz region for the ^{35}Cl species and 11 for ^{37}Cl. The line centers were fitted to obtain ground state rotational and quartic centrifugal distortion constants A'', B'', C'', τ_1, τ_2, τ_{aaaa}, τ_{bbbb}, and τ_{cccc}. For Ar_2–$H^{35}Cl$, the values are 1733.857, 1667.932, 844.491, -0.1170, -0.0292, -0.1199, -0.0802, and -0.0079 MHz, respectively, and for Ar_2–$H^{37}Cl$: 1733.824, 1606.877, 828.497, -0.1121, -0.0279, -0.1205, -0.0737, and -0.0075 MHz. The equilibrium geometry is determined to be T shaped with C_{2v} symmetry and the H end of the HCl closest to the Ar_2. Large amplitude slightly anisotropic torsional motion of the HCl is evident from the hyperfine constants. The chlorine isotopic substitution enables the torsional displacement of the Ar_2 dimer to be estimated. It is found to be an average of 7.3° with respect to the *b* axis. With allowance for the torsional effects, a value of 3.861 Å is obtained for the Ar–Ar distance and 4.005 Å for the Ar to Cl distance. An approximate, harmonic force field analysis is based on the centrifugal distortion constants. A comparison is given of the force constants and Ar–Ar distances for the Ar_2–HCl and Ar_2–H/DF trimers.

I. INTRODUCTION

The rotational spectrum of the Ar–HCl van der Waals molecule was first reported in 1973.[1] A linear geometry was established with the hydrogen weakly bound to the noble gas atom. Since then, molecular beam electric resonance and pulsed nozzle Fourier transform microwave spectroscopy have been used to determine rotational constants, structure, and dynamics for the ground vibrational state of many other binary complexes of noble gas atoms with species having acidic hydrogen. A few such examples are Ar–HF, Kr–HF, Kr–HCl, Xe–HCl, and Ar–HCN.[2] In each case the equilibrium geometry has the proton linearly bound between the two heavier atoms. Also, for the ground vibrational state, large amplitude isotropic libration of the HX group is the rule.

Recently, microwave spectra were reported for the small clusters Ar_2–HF[3] and Ar_3–HF.[4] In addition to being the first such microwave studies of complexes larger than dimers, they are the first cases of a "nonlinear" van der Waals bond between proton and noble gas atom. Also, the work demonstrated the feasibility of studying the pure dispersion forces between noble gas atoms by means of rotational microwave spectroscopy. The Ar_2–HF trimer was found to be T shaped and at equilibrium the H is most likely pointing between the two argons in the Ar_2 subunit. Similarly, the Ar_3–HF cluster is a symmetric top with the H of the HF pointed inwards along the C_3 axis. In both cases, there is large amplitude zero-point libration of the hydrogen. A pseudotriatomic model was applied to the centrifugal distortion constants of Ar_2–HF to give an estimate of the attractive forces holding the complex together.

We now report the microwave spectrum of the HCl analog to the Ar_2–HF complex, as observed with a Balle–Flygare spectrometer.[5] As in previous studies of van der Waals complexes the clusters are formed during a pulsed-nozzle gas expansion. Typically, a carrier noble gas seeded with 1% of the hydrogen halide is held at a pressure of 1 atm prior to expansion. It is known from mass spectra[6] that in addition to the simple dimers Ar_2, Ar–HCl, and $(HCl)_2$, the higher order complexes Ar_m, Ar_m–$(HCl)_n$ are formed during the expansion in concentrations decreasing with increasing *m* and *n*. Complexes consisting of argon alone, Ar_m with $m = 2,3,4,...$, have little or no dipole moment and are not detectable via rotational spectroscopy. However, the mixed species Ar_m–HCl do have microwave spectra. These species may be viewed as Ar_m clusters with an HCl molecule attached acting as a dipole handle. This allows a study of the structure of small noble gas clusters, albeit perturbed by a polar unit. We may now address such questions as the dependence of the Ar–Ar distance on cluster size and on the nature of the HX group in Ar_m–HX, or we can compare attractive forces. In the present case, the existence of two chlorine isotopes enables us to make a more detailed structural analysis of the trimer, including the in-plane torsion of the Ar_2.

II. EXPERIMENTAL

The Flygare spectrometer combines the principles of pulsed Fourier transform spectroscopy, a Fabry–Perot cavity, and synchronization of the microwave pulse with supersonic expansion of a pulsed beam of a gas mixture.[5] The expansion cools the gas mixture, generates the weak molecular complexes, and gives rotational temperatures of ~5 K. Initially, we used argon as the carrier gas and seeded it with ~1% HCl (Matheson). In this case optimum signal

0021-9606/87/105315-08$02.10

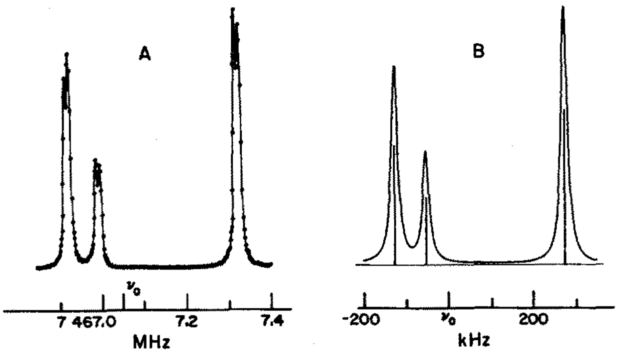

FIG. 1. Central portion of the hyperfine structure for the $3_{03}\rightarrow 4_{04}$ transition of Ar_2–$H^{37}Cl$ at 7467.052 MHz showing three strong $\Delta F = 1$ components. (A) Observed in 1.5 min by averaging 663 FID's digitized at 300 ns for 512 points, giving a resolution of 1.628 kHz/point. The doublets are caused by Doppler splitting. (B) Simulated best fit (see Table I).

strength was obtained for the Ar_2–HCl complex at a total pressure P_0 of 0.831 atm behind the 1.0 mm diameter nozzle. Later, an improved method for making these small clusters was developed.

The method uses neon "first run" (Airco Gas) as a carrier gas (70% Ne, 30% He) with a small fraction of Ar and an even smaller amount of HCl. Optimum signal strength for the trimer occurred at $P_0 \approx 2$ atm with about 15% Ar, 0.5% HCl, in 85% neon first run. With the first run carrier gas, a larger pulse of gas (longer opening of the nozzle) was required for optimum generation of the complex. Generally, the signal strength was fourfold larger than with argon as the carrier. This method is most advantageous at lower frequencies (less than 10 GHz) where Doppler broadening is minimal and for systems where there is no hyperfine structure (hfs) or where the components are separated by more than the Doppler splitting (50 kHz or more). It would not be recommended for resolving deuterium hyperfine structure.

The operating range of the Mark II spectrometer[7] was extended to S band (2–4 GHz) in order to see the $J = 0$ to $J = 1$ transition of Ar_2–$H^{35}Cl$. As with C band[8] a dipole was used to couple radiation into and out of the cavity. In the data collection a given hyperfine component (or set of them) was averaged at an overall repetition rate of 8 Hz on an LSI-11. After suitable accumulation of signal, the free induction decay (FID) was transformed into the frequency spectrum. This was repeated several times so that an average line frequency and standard deviation could be determined. For well-resolved lines with good S/N, the standard deviation was typically 1 kHz.

III. RESULTS AND ANALYSIS

A. Transition frequencies and hyperfine structure

The search for the Ar_2–HCl complex was straightforward. Using the Ar_2–HF findings as a guide, we calculated the rotational constants and spectrum for a symmetric T-shaped complex with an Ar to Cl distance as determined for Ar–HCl[1] and an Ar to Ar distance as found in Ar_2–HF.[3] The calculated spectrum is that of an oblate near symmetric top with the HCl lying along the a axis. (In Ar_2–HF, the HF is along the b axis.) The search began in low C band at 4.2 GHz, a region predicted to be cluttered with lines. The method described in the experimental section was used to determine the frequency for several of the main (and sometimes minor) hyperfine components for each rotational transition. The transitions were identified by means of their hyperfine structure. An example is given in Fig. 1 which shows the three central $\Delta F = +1$ components of the $3_{03}\rightarrow 3_{04}$ transition of Ar_2–$H^{37}Cl$. After several transitions had been located and assigned, their line centers were fitted to obtain better rigid-rotor rotational constants and more accurate predictions to guide the search for additional transitions.

The hfs observed for 16 transitions of Ar_2–$H^{35}Cl$ is summarized in Table I and for 11 transitions of Ar_2–$H^{37}Cl$ in Table II. Its analysis is very similar to that made of Ar_2–H/DF.[3] Spin–rotation interaction and the small H–Cl dipole–dipole interaction (10 kHz) were neglected so the Hamiltonian

$$H = H_R + H_Q \tag{1}$$

consisted of only the rotational (H_R) and the chlorine quadrupole interaction (H_Q) terms. The matrix elements of H were calculated using the coupled basis set $F = J + I$, where $I = 3/2$ for both chlorine isotopes. The trimer has C_{2v} symmetry so for H_Q the off-diagonal elements of χ_{gg} are zero ($g = a,b,c$). However, the torsional oscillations of HCl are anisotropic so both χ_{aa} and $(\chi_{bb} - \chi_{cc})/\sqrt{6}$ were used as adjustable parameters in the fit. An asymmetric top hyperfine fitting program good through the second order was employed. Approximate rotational constants were used for fitting the hfs so the apparent position of the line center was also a fitted parameter. The fitting was performed for several transitions at a time, with the results given in Tables I and II. The hyperfine interaction constants obtained in this manner were averaged for each isotopic species. These results are listed in Table III. The quality of the fit is comparable with that reported for the T shaped acetylene–HCl complex.

The line centers found for the Ar_2–HCl complexes are listed in Table IV. These frequencies were fitted to Kirchoff's CDANAL computer program for the distortable asymmetric rotor.[9] With it we evaluated the Watson determinable parameters,[10] i.e., the three rotational constants, and five centrifugal distortion constants through fourth order (tau's). The results are listed in Table V along with several other "molecular" properties derived from them. The fit of the line centers with an rms deviation of 2.5 kHz is almost as good as that for Ar_2–H/DF which included three sixth order terms, so the latter were not employed here. The correlation coefficients for the fits are comparable with those for Ar_2–H/DF. Only 5 of the 36 off-diagonal coefficients exceed 0.5 in magnitude; the largest (~ -0.8) are for A'', B'', and C'' with the corresponding τ_{gggg}.

B. Molecular symmetry

With the results for Ar_2–H/DF to draw upon, it is readily apparent that Ar_2–HCl is also a T shaped complex with C_{2v} symmetry (Fig. 2). From the value of the asymmetry parameter κ (0.852) for Ar_2–$H^{35}Cl$, it is seen that the complex is an oblate near symmetric top. This is consistent with a

TABLE I. Observed and fitted hyperfine components for the rotational transitions of Ar_2–$H^{35}Cl$.[a]

Transition $J_{K_pK_0}\to J'_{K_pK_0}$	Component $F\to F'$	Observed (MHz)	Obs. – Calc. (kHz)
$0_{00}\to 1_{01}$	3/2→3/2	2 506.723	4
	3/2→5/2	2 513.750	– 4
(A) – 28.149(17)			
– 1.288(5)			
$1_{01}\to 2_{02}$	1/2→3/2	4 256.193	– 3
	5/2→5/2	4 258.743	0
(B) – 28.106(6)	1/2→1/2	4 260.475	– 4
– 1.303(5)	5/2→7.2	4 263.041	0
	3/2→5/2	4 265.772	4
	3/2→3/2	4 268.848	2
$1_{01}\to 2_{20}$	1/2→1/2	7 684.604	1
	5/2→7/2	7 693.287	3
(B)	5/2→5/2	7 697.578	– 7
	3/2→3/2	7 701.541	6
	3/2→5/2	7 704.606	– 3
$3_{03}\to 3_{22}$	9/2→9/2	4 281.802	3
	5/2→5/2	4 284.466	– 3
(A)	7/2→7/2	4 286.815	– 1
$2_{02}\to 3_{03}$	7/2→7/2	5 919.519	0
	3/2→5/2	5 923.082	1
(B)	1/2→3/2	5 923.815	0
	5/2→7/2	5 923.815	– 1
	7/2→9/2	5 924.534	3
	5/2→5/2	5 926.154	– 5
	3/2→3/2	5 928.101	2
$2_{21}\to 3_{22}$	5/2→7/2	7 531.045	– 1
	3/2→5/2	7 536.063	– 2
(B)	7/2→9/2	7 538.073	2
	1/2→3/2	7 543.098	1
$2_{02}\to 3_{21}$	1/2→3/2	12 577.976	– 1
	7/2→7/2	12 578.069	– 3
(A)	7/2→9/2	12 580.089	0
	3/2→5/2	12 580.230	– 3
	3/2→3/2	12 582.264	5
	5/2→7/2	12 582.373	3
$2_{20}\to 3_{21}$	5/2→7/2	9 143.535	– 2
	3/2→5/2	9 147.545	– 2
(C) – 28.138(26)	3/2→3/2	9 149.569	4
– 1.317(14)	7/2→9/2	9 149.847	1
$3_{03}\to 4_{04}$	9/2→9/2	7 605.495	– 3
	5/2→7/2	7 610.119	– 2
(B)	7/2→9/2	7 610.510	0
	3/2→5/2	7 610.673	0
	9/2→11/2	7 611.063	1
	7/2→7/2	7 612.464	1
	5/2→5/2	7 615.693	2
$3_{22}\to 4_{23}$	7/2→9/2	9 312.317	0
	5/2→7/2	9 312.895	– 2
(C)	9/2→11/2	9 313.968	1
$3_{21}\to 4_{22}$	3/2→5/2	11 174.331	1
	9/2→11/2	11 175.287	8
(C)	5/2→7/2	11 176.356	– 2
	7/2→9/2	11 177.289	– 7
$3_{21}\to 4_{40}$	3/2→5/2	14 702.215	10
	9/2→11/2	14 705.108	4
(B)	5/2→7/2	14 709.798	– 4
	7/2→9/2	14 712.694	– 9
$4_{04}\to 5_{05}$	7/2→9/2	9 298.512	2
	9/2→11/2	9 298.788	– 1
(C)	5/2→7/2	9 298.886	1
	11/2→13/2	9 299.163	– 1
$4_{22}\to 5_{23}$	9/2→11/2	12 749.344	– 5
	7/2→9/2	12 749.392	– 4
(B)	11/2→13/2	12 749.438	6
	5/2→7/2	12 749.468	3
$4_{41}\to 5_{42}$	9/2→11/2	14 100.838	– 7
	7/2→9/2	14 103.157	– 3
(B)	11/2→13/2	14 106.948	4
	5/2→7/2	14 109.268	6
$4_{40}\to 5_{41}$	9/2→11/2	15 617.625	1
	7/2→9/2	15 619.854	– 1
(B)	5/2→7/2	15 626.392	1

[a] The components were fitted for several transitions at a time. The groups are lettered and the values in MHz obtained for χ_{aa} and $(\chi_{bb}-\chi_{cc})/\sqrt{6}$ are given in that order just below the designation of the first transition for each group. Numbers in parentheses are the standard deviation in the last digit(s).

T geometry where the closeness in mass of the HCl (36) and Ar (40) and of their van der Waals radii give a near C_3 distribution of the mass, with rotational constants $A\cong B\cong 2C$. Furthermore, the value found for A'' in the Ar_2–HCl trimers (1734 MHz) is very close to B'' of Ar_2–HF (1739 MHz) and to B_0 of Ar_2 (1732 MHz),[11] and the rotational transitions observed are *a* and *b* dipole, respectively, for the two trimers. Finally, all of the transitions found (Table IV) are between $J_{K_pK_0}$ states one of which has K_pK_0 even–even (ee) and the other even–odd (eo); none are oo↔oe. Equal numbers of the two types of rotational transitions are predicted for an *a* dipole asymmetric top without a symmetry axis. However, the oo and oe states are prohibited by the Bose–Einstein statistics when the *a* axis is a twofold axis interchanging identical $I=0$ nuclei (^{40}Ar).[12]

C. Vibrational modes and torsional effects

Of the forces holding the Ar_2–HCl cluster together, only the H–Cl interaction is a strong bond. The Ar–Ar and Ar–HCl interactions are weak ($\sim 150\ \mathrm{cm}^{-1}$), and the corresponding vibrational amplitudes are large. This shows up in the large inertial defects, $\Delta = 3.968$ and 4.002 amu Å^2 for the $H^{35}Cl/^{37}Cl$ species (Table V). The positive values of Δ indicate that out-of-plane vibrational effects are small.

Six internal coordinates may be used to describe the six vibrational modes of the cluster—the two torsional angles θ_b and θ_c of the HCl, the in-plane torsional angle β of the Ar_2, the Ar–Ar distance (r), the Ar_2 c.m. to HCl c.m. distance (R), and the $H^{35}Cl/^{37}Cl$ bond length (Fig. 2). Cluster formation perturbs the H–Cl stretch by only a small amount so we neglect it. Vibrational averaging of r and R probably affects the moments of inertia the most, but it is difficult to evaluate. An estimate of the Ar_2 torsional oscillations (β) is made later by an inertial analysis of the $^{35}Cl/^{37}Cl$ isotopic species in connection with the structural determination. Here we consider libration of the HCl (θ_b and θ_c), which can be determined from the chlorine quadrupole coupling.

Free HCl, the properties of which are listed in Table VI, exhibits hfs described by the ^{35}Cl or ^{37}Cl quadrupole cou-

TABLE II. Observed and fitted hyperfine components for the rotational transitions of Ar_2–$H^{37}Cl$.[a]

Transition $J_{K_pK_o} \rightarrow J'_{K_pK_o}$	Component $F \rightarrow F'$	Observed (MHz)	Obs − calc (kHz)
$1_{01} \rightarrow 2_{02}$	1/2→3/2	4 199.181	2
	5/2→5/2	4 200.997	0
(A) −22.199(4)	1/2→1/2	4 202.833	−3
− 1.019(3)	5/2→7/2	4 204.662	−2
	3/2→5/2	4 206.548	2
	3/2→3/2	4 209.171	1
$1_{01} \rightarrow 2_{20}$	1/2→3/2	7 594.664	2
	5/2→7/2	7 598.060	2
(B) −22.202(3)	5/2→5/2	7 601.724	−2
− 1.033(16)	3/2→5/2	7 607.273	−1
$2_{02} \rightarrow 3_{03}$	7/2→7/2	5 813.297	−1
	3/2→5/2	5 816.235	0
(A)	1/2→3/2	5 816.640	4
	5/2→7/2	5 816.962	−3
	7/2→9/2	5 817.355	2
	5/2→5/2	5 818.856	−3
	3/2→3/2	5 820.295	+2
$2_{21} \rightarrow 3_{22}$	5/2→7/2	7 301.015	+2
	5/2→5/2	7 301.015	−2
(B)	3/2→5/2	7 304.979	−1
	7/2→9/2	7 306.564	1
	1/2→3/2	7 310.531	0
$2_{20} \rightarrow 3_{21}$	5/2→7/2	8 789.236	1
	7/2→9/2	8 794.393	0
(C) −22.203(9)	1/2→3/2	8 797.704	−1
−1.025(30)			
$3_{03} \rightarrow 4_{04}$	9/2→9/2	7 462.869	−2
	5/2→7/2	7 466.595	0
(A)	7/2→9/2	7 466.927	1
	3/2→5/2	7 466.997	0
	9/2→11/2	7 467.328	0
	7/2→7/2	7 468.490	0
	5/2→5/2	7 471.057	2
$3_{22} \rightarrow 4_{23}$	7/2→9/2	9 116.187	−1
(A)	9/2→11/2	9 117.664	0
$3_{21} \rightarrow 4_{40}$	9/2→11/2	14 769.737	1
	5/2→7/2	14 774.049	−1
(D) −22.178(18)	7/2→9/2	14 776.649	1
− 1.025(20)			
$4_{04} \rightarrow 5_{05}$	7/2→9/2	9 122.529	−1
	9/2→11/2	9 122.761	2
(C)	5/2→7/2	9 122.812	0
	11/2→13/2	9 123.039	−1
$4_{22} \rightarrow 5_{23}$	5/2→7/2	12 579.180	−4
	11/2→13/2	12 579.367	4
(D)	7/2→9/2	12 579.586	2
	9/2→11/2	12 579.765	−1
$5_{24} \rightarrow 6_{25}$	11/2→13/2	12 456.080	−2
	9/2→11/2	12 456.104	−1
(D)	7/2→7/2	12 456.619	3

[a] The components were fitted for several transitions at a time. The groups are lettered and the values in MHz obtained for χ_{aa} and $(\chi_{bc} - \chi_{cc})/\sqrt{6}$ are given in order just below the designation of the first transition for each group. Numbers in parentheses are the standard deviation in the last digit(s).

pling constant χ_0. For it χ_0 coincides with χ_{aa}; moreover, by symmetry and the condition $\Sigma_g \chi_{gg} = 0$ $(g = a,b,c)$, one has $\chi_{bb} = \chi_{cc} = -\chi_0/2$. If the electrical properties of HCl are unperturbed by complex formation, an assumption which has been shown to be good for noble gas–hydrogen halide complexes,[14] then in nonvibrating, C_{2v} Ar_2–HCl the measured χ_{gg}'s should agree with those of free HCl, with χ_0 along the *a* axis of the trimer. However, the measured χ's are projections of χ_0 upon the inertial axes of the complex, vibrationally averaged over the large amplitude zero-point motion of the HCl. Analysis of the averaging is the same as that employed for the T shaped acetylene–HCl dimer.[15] It defines the average angular displacement of the HCl from the *a* axis in the *ab* and *ac* planes (Fig. 2) to be, respectively,

$$\theta_b = \left[\frac{\chi_{aa} + (\chi_0/2)}{\chi_{aa} + \chi_{bb} + \chi_0} \right]^{1/2} \tag{2a}$$

and

$$\theta_c = \left[\frac{\chi_{aa} + (\chi_0/2)}{\chi_{aa} + \chi_{cc} + \chi_0} \right]^{1/2}. \tag{2b}$$

Applying Eq. (2) to the data on χ_{gg} (Table III) we find for Ar_2–$H^{35}Cl$ a θ_b of 30.40° and a θ_c of 28.43°. The results for the $H^{37}Cl$ species are virtually identical, 30.39° and 28.42°. There is a 2° anisotropy in the torsion with the in-plane oscillation favored. The in- and out-of-plane angles correspond to an average, overall angle γ between the *a* axis and the HCl axis of 38.6°.

D. Structural analysis

By treating the Ar_2 and HCl torsion as in-plane (*ab* and *ac*) motion we may write the moments of inertia for the trimer as[3]

$$I_A = I_{Ar_2} \langle \cos^2 \beta \rangle + I_{HCl} [\langle \sin^2 \theta_b \rangle + \langle \sin^2 \theta_c \rangle], \tag{3a}$$

$$I_B = \mu_c R^2 + I_{HCl} \langle \cos^2 \theta_b \rangle + I_{Ar_2} \langle \sin^2 \beta \rangle, \tag{3b}$$

$$I_C = \mu_c R^2 + I_{Ar_2} + I_{HCl} \langle \cos^2 \theta_c \rangle, \tag{3c}$$

where μ_c is the reduced mass of the complex treated as pseudodiatomic with Ar_2 and HCl components, *R* is the distance between Ar_2 and HCl centers of mass, and I_{HCl} and I_{Ar_2} are the moments of inertia of free HCl (Table VI) and of Ar_2 in the complex. The Ar–Ar distance *r* is defined by $I_{Ar_2} = (M_{Ar}/2)r^2$. Application of Eq. (3) to analyze the structure of Ar_2–HCl closely follows the procedures used for Ar_2–H/DF. However, the availability of results for the two more similar chlorine isotopes enables a more detailed analysis to be made of the Ar_2 torsion. A conversion factor of 505 379.0 amu Å^2 MHz was used for $I \times B$. The inertial properties of the two trimers are listed in Table VII.

Because of the large inertial defect, the redundancy in Eq. (3) leads to substantial differences (~0.025 Å) in the two values of *r* and *R* obtainable from I_A and $(I_C - I_B)$ and from I_B and $(I_C - I_A)$, respectively. We average them by using the planar moments, $P_A = (1/2)(I_B + I_C - I_A)$ and P_B and P_C defined by cyclic permutation. Initially, we neglect the torsional oscillations, setting β, θ_b, and θ_c equal to zero in Eq. (3). This leads to $P_A = \mu_c R^2 + I_{HCl}$, $P_B = I_{Ar_2}$, $P_C = -\frac{1}{2}\Delta$, and gives values for *R* and *r* of 3.4969 and 3.8323 Å in Ar_2–$H^{35}Cl$ and of 3.4975 and 3.8325 in Ar_2–$H^{37}Cl$. Inclusion of the HCl torsion with θ_b and θ_c from the quadrupole coupling (Table III) decreases the apparent Ar–Ar distance *r* by 0.0027 Å and increases the pseudodiatomic *R* by 0.0044 Å as shown in Table VIII.

TABLE III. Hyperfine interaction constants and torsional amplitudes found for the HCl in Ar_2–$H^{35}Cl$ and Ar_2–$H^{37}Cl$.

Isotopic species	χ_{aa} (MHz)	χ_{bb} (MHz)	χ_{cc} (MHz)	θ_b (deg)	θ_c (deg)	γ (deg)
Ar_2–$H^{35}Cl$	− 28.123(14)	12.471(13)	15.658(13)	30.40(1)	28.43(1)	38.60
Ar_2–$H^{37}Cl$	− 22.201(5)	9.844(21)	12.356(21)	30.39(1)	28.42(1)	38.59

TABLE IV. Observed and fitted line centers for the rotational transitions of Ar_2–$H^{35}Cl$ and Ar_2–$H^{37}Cl$.

	Ar_2–$H^{35}Cl$		Ar_2–$H^{37}Cl$	
Transition $J_{K_pK_o} \rightarrow J'_{K_pK_o}$	Obs. (MHz)	Obs. − Calc. (kHz)	Obs. (MHz)	Obs.–Calc. (kHz)
$0_{00} \rightarrow 1_{01}$	2 512.344	1		
$1_{01} \rightarrow 2_{02}$	4 263.227	7	4 204.727	0
$1_{01} \rightarrow 2_{20}$	7 695.914	− 2	7 600.216	0
$3_{03} \rightarrow 3_{22}$	4 283.470	0		
$2_{02} \rightarrow 3_{03}$	5 924.082	− 4	5 817.047	1
$2_{21} \rightarrow 3_{22}$	7 536.064	3	7 304.977	1
$2_{02} \rightarrow 3_{21}$	12 580.642	0		
$2_{20} \rightarrow 3_{21}$	9 147.947	1	8 792.848	− 1
$3_{03} \rightarrow 4_{04}$	7 610.706	− 1	7 467.052	− 4
$3_{22} \rightarrow 4_{23}$	9 313.367	− 2	9 117.129	2
$3_{21} \rightarrow 4_{22}$	11 175.955	− 4		
$3_{21} \rightarrow 4_{40}$	14 707.822	0	14 772.203	− 1
$4_{04} \rightarrow 5_{05}$	9 298.901	1	9 122.837	3
$4_{22} \rightarrow 5_{23}$	12 749.386	5	12 579.497	1
$4_{41} \rightarrow 5_{42}$	14 104.776	− 5		
$4_{40} \rightarrow 5_{41}$	15 621.761	1		
$5_{24} \rightarrow 6_{25}$			12 456.355	0

TABLE V. Watson's determinable parameters[10] obtained by using the Kirchhoff program[9] with fourth-order centrifugal distortion to fit the line centers found for Ar_2–$H^{35}Cl$ and Ar_2–$H^{37}Cl$, with molecular constants derived from these parameters.

Quantity	Ar_2–$H^{35}Cl$	Ar_2–$H^{37}Cl$
	Watson's determinable parameters[a]	
A'' (MHz)	1733.857 1(15)	1733.824 4(13)
B''	1667.932 2(8)	1606.876 6(15)
C''	844.490 8(7)	828.497 4(5)
τ_1	− 0.117 0(2)	− 0.112 1(4)
τ_2	− 0.029 15(8)	− 0.027 9(1)
τ_{aaaa}	− 0.119 9(4)	− 0.120 5(4)
τ_{bbbb}	− 0.080 2(1)	− 0.073 7(6)
τ_{cccc}	− 0.007 86(8)	− 0.007 49(7)
	Derived molecular constants[b]	
Δ (amu Å^2)[a]	3.968 2(5)	4.002 2(5)
τ_{aabb} (MHz)	0.038 8(5)	0.037 2(5)
τ_{abab}	− 0.061 8(4)	− 0.059 3(4)
F_{11} (10^{-5} dyn/Å)	1.651	1.658
F_{12}	0.566	0.562
F_{22}	0.683	0.679
F_{33}	1.089	1.093

[a] Uncertainties are the standard deviation.

[b] The uncertainties in the τ's are the rms deviation of the three values averaged.

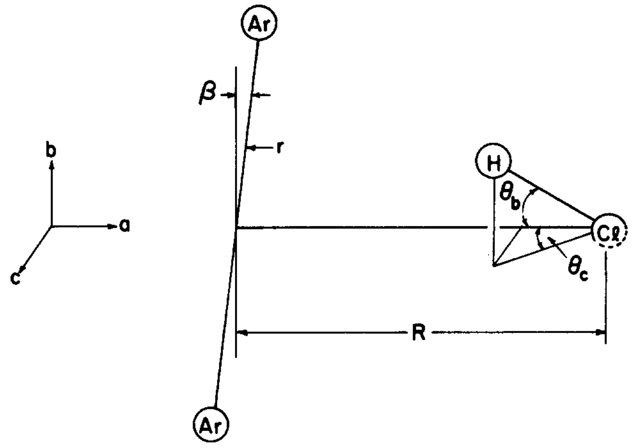

FIG. 2. Geometrical structure and inertial axes of the Ar_2–HCl trimer. The atomic positions are drawn to scale; θ_b and θ_c are the average angles between the *a* axis and the HCl axis projected onto the *ab* and *ac* inertial planes, and *R* is the Ar_2 c.m. to HCl c.m. distance.

TABLE VI. Spectroscopic and structural properties of free $H^{35}Cl$ and $H^{37}Cl$.[a]

Property	Units	$H^{35}Cl$	$H^{37}Cl$
B_0	MHz	312 989.297	312 510.121
r_0	Å	1.283 87	1.283 86
χ_0 (Cl)	MHz	− 67.618 9	− 53.294
$\delta r_{c.m.}$[b]	Å	0.035 97	0.034 07

[a] See Ref. 13.

[b] This is the distance from the HCl c.m. to the chlorine nucleus.

TABLE VII. Inertial properties for the Ar_2–HCl trimers.

Species	I_A (amu Å^2)	I_B (amu Å^2)	I_C (amu Å^2)	μ_c (amu)
Ar_2–$H^{35}Cl$	291.476 7(3)	302.997 3(1)	598.442 3(5)	24.809 25
Ar_2–$H^{37}Cl$	291.482 2(2)	314.510 2(3)	609.994 7(4)	25.742 83

The extent of the Ar_2 torsion may be approximated by subtracting the terms in I_{HCl} from the numerical and algebraic values for the moments of inertia and planar moments. In this way we obtain expressions such as

$$I'_A = I_A(\text{obs}) - I_{HCl}\left[\langle \sin^2\theta_b\rangle + \langle \sin^2\theta_c\rangle\right] = I_{Ar_2}\langle \cos^2\beta\rangle, \qquad (4)$$

TABLE VIII. Distances within the T shaped Ar_2–$H^{35}Cl$ and Ar_2–$H^{37}Cl$ with and without inclusion of $H^{35}Cl$/^{37}Cl and Ar_2 torsional effects.

Parameter[a] (Å)	Ar_2–$H^{35}Cl$			Ar_2–$H^{37}Cl$		
	None	HCl	HCl/Ar_2[b]	None	HCl	HCl/Ar_2[b]
r	3.8323	3.8296	3.8611	3.8325	3.8298	3.8612
R	3.4969	3.5013	3.4734[c]	3.4975	3.5018	3.4749[c]
R_0	3.5329	3.5373	3.5094	3.5316	3.5359	3.5090
d	3.9875	3.9907	3.9739	3.9880	3.9912	3.9752
d_0	4.0191	4.0223	4.0054	4.0180	4.0211	4.0050

[a] The distances are: r, Ar-Ar; R, Ar_2 c.m. to HCl c.m.; d, Ar to HCl c.m.; the zero subscript indicates distances to the Cl nucleus instead of the HCl c.m.

[b] Based on an average Ar_2 torsional angle $\beta = 7.32°$.

[c] The difference between the ^{35}Cl and ^{37}Cl species was imposed.

from which

$$P'_A = \tfrac{1}{2}(I'_B + I'_C - I'_A) = I_{Ar_2}\langle \sin^2\beta \rangle + \mu_c R^2 \quad (5)$$

and

$$P'_B = I_{Ar_2}\langle \cos^2\beta \rangle. \quad (6)$$

A numerical value is obtained for R by subtracting P'_A for the ^{35}Cl complex from that for ^{37}Cl, with allowance for the 0.0015 Å difference in R caused by the isotopic displacement of 0.0019 Å in the HCl c.m. and its projection by cos γ on the a axis. This analysis depends on small differences between large numbers and is sensitive to the value used for the isotopic difference in R. With R in hand, the ratio and sum of P'_A and P'_B give the averaged values of β and of r for each isotopic species. The result for β is 7.32°. Inclusion of the Ar_2 torsion in this manner increases r by about 0.03 Å, and decreases R by almost as much. The values are given in Table VIII along with the Ar to HCl c.m. distance d and the distances between argon and the chlorine nuclei derived from r and R for the equilibrium configuration.

There remains the question of the HCl orientation in the trimer. For the Ar–HX dimers and the Ar_2–HF trimer the H end is closest to the argons. We find this also to be the case for Ar_2–HCl. The most direct evidence is the difference in R between the $H^{35}Cl$ and $H^{37}Cl$ complexes. If the Cl is outside of the HCl c.m., substitution of ^{37}Cl for ^{35}Cl moves the HCl c.m. away from the Ar_2 and increases R; otherwise the reverse is true. Actually, we find that R for Ar_2–$H^{37}Cl$, when torsional effects of the Ar_2 are not included, is 0.0006 Å larger than for Ar_2–$H^{35}Cl$ (Table VIII). This is less than predicted (Table VI), but it is in the right direction. The analysis of the Ar_2 torsion also supports the Ar_2–HCl configuration. It assumes R for Ar_2–$H^{37}Cl$ to be 0.0015 Å longer than for Ar_2–$H^{35}Cl$, an assumption which gives reasonable results for r and β. However, the reverse assumption gives larger values for R, which lead to physically unreasonable negative values (-9 amu Å^2) for $I_{Ar_2}\langle \sin^2\beta \rangle$.

The position of the chlorine in the trimer can also be determined by applying Kraitchman's isotope substitution method[16] to the differences in the moments of inertia for the $H^{35}Cl$ and $H^{37}Cl$ complexes. Thereby we have

$$\Delta P'_A = \mu_s a^2, \quad (7)$$

where μ_s is the reduced mass for the substitution and a is the distance along the a axis from the chlorine to the c.m. of the complex. Our data give $a = 2.4234$ Å. The $H^{35}Cl$ c.m. is 0.0281 Å from the torsional projection (0.0360 Å cos γ) of the ^{35}Cl on the a axis. The resulting separation between the c.m. of HCl and that of the complex gives an R_s for ^{35}Cl of 3.4735 Å. The value of R determined by the more detailed torsional analysis is 3.4734 Å (Table VIII). The fitting process constrains the results for Ar_2–$H^{37}Cl$ to be equally good.

E. Force field

An approximate analysis of the forces in the Ar_2–HCl cluster can be based upon the centrifugal distortion constants, following the procedure adopted for Ar_2–H/DF.[3] In a planar molecule three of the five determinable τ's (Table V) reduce to two (τ_{aabb},τ_{abab}). The values obtained for the latter vary by 10%, depending on which pair of the three τ's (τ_1,τ_2,τ_{cccc}) is used in the reduction.[9] Their averages, given in Table V, and the "determinable" constants τ_{aaaa} and τ_{bbbb} were employed for the analysis. In order to simplify the analysis, a pseudotriatomic model is used in which libration of the HCl is neglected, i.e., the HCl is treated as a point mass at its center of mass. The other structural features needed are taken from this study.

The evaluation of the force constants is like that made earlier on bent XY_2 covalent molecules such as SO_2 and OF_2.[9] The internal coordinates are the Ar to HCl c.m. distance d and the Ar to HCl c.m. to Ar angle α. The three symmetry coordinates

$$s_1 = \frac{1}{\sqrt{2}}(\Delta d_1 + \Delta d_2), \quad (8a)$$

$$s_2 = d\Delta\alpha, \quad (8b)$$

$$s_3 = \frac{1}{\sqrt{2}}(\Delta d_1 - \Delta d_2), \quad (8c)$$

are used along with the expressions giving the four elements of the inverse force constant matrix (F^{-1}) in terms of the four planar tau's. The expressions were modified to allow for the different orientation of a and b inertial axes in Ar_2–HCl. The inversion of the matrix yields the force constant elements F_{11}, F_{12}, F_{22}, and F_{33} listed in Table V. They are retained in terms of the symmetry coordinates, which may be

TABLE IX. Comparison of force constants derived for the Ar and Ar_2 complexes of HCl and H/DF.

Complex	Force constant	Ar_m–HCl[a] (10^{-5} dyn/Å)	Ar_m–HF (10^{-5} dyn/Å)	Ar_m–DF (10^{-5} dyn/Å)
Ar–HX[b]	f_R	1.17	1.47	1.79
Ar_2–HX[c]	F_{11}, f_R	1.66	1.86	1.97
	F_{12}, f_{Rr}	0.56	0.62	0.64
	F_{22}, f_r	0.68	0.66	0.68
	$F_{33}, 4f_\beta$	1.09	1.08	1.06

[a] Averaged for the ^{35}Cl and ^{37}Cl species.

[b] Pseudodiatomic model; see Ref. 18.

[c] Pseudotriatomic model; see Ref. 3.

identified more readily with the structural parameters of the complex. F_{11} describes the stretch in the distance R between the two centers of mass. F_{22} in the typical triatomic is identified with the X–Y–X angle bending force constant but here may be attributed to the Ar–Ar stretch (r). F_{12} is a sizeable interaction constant between the stretches in R and r. F_{33}, an asymmetric stretch in the Ar to HCl c.m. distances, is equivalent to the Ar_2 torsion.

IV. DISCUSSION

The high sensitivity and resolution afforded by pulsed nozzle Fourier transform microwave spectroscopy has allowed identification and characterization of the Ar_2–HCl trimer. Our findings fit in well with the present understanding of rare gas–hydrogen halide complexes. The torsional angles determined for HCl in the trimer agree with those in Ar–HCl. There, the average angle between HCl and the linear axis was found to be 41.53°, also determined from the Cl nuclear hfs. The libration in Ar–HCl is isotropic with an angle in each of the two degenerate planes of 32.06°. In Ar_2–HCl, the average angle is slightly smaller (38.60°) than the 41.53° in Ar–HCl. Now, however, anisotropy in the torsion occurs, with an in-plane-of-complex angle of 30.40° and an out-of-plane angle of 28.42°. This is consistent with our findings for Ar_2–HF, where an in-plane angle of 32.8° and an out-of-plane angle of 29.7° were determined. The anisotropy of only 2° or 3° indicates that the potential function between Ar_2 and HX has close to axial symmetry in the trimers, at least for the ground state, in spite of the large separation between the two argons. Another point worth noting is that the argon to HCl c.m. to argon angle is 58.1°. The half-angle of 29° is virtually identical with the in-plane torsional angle of 28.4°. Therefore, the HCl is on the "average" pointed at one or the other of the Ar atoms.

The internuclear distances for Ar_2–HCl appear to be very reasonable. A high resolution absorption spectrum of argon by Colbourn *et al.*[11] reported B_0 to be 0.057 78(30) cm^{-1} for the dimer (Ar_2). This corresponds to an r_0 of 3.821(10) Å. Presently, using the model which takes into account both the HCl and Ar_2 torsion, we arrive at an Ar–Ar separation of 3.861 Å. The effect of the Ar_2 torsional angle β is to increase the apparent argon–argon distance through the $\langle \sin^2\beta \rangle$ and $\langle \cos^2\beta \rangle$ terms in I_A and I_B, Eq. (3). For Ar–HCl, an Ar to Cl distance of 4.006 Å was reported.[1] In Ar_2–HCl this distance has been determined to be 4.005 Å (Table VIII), which is the same within model error. Furthermore, the Ar to Cl distance has been determined to be 4.002 Å in the Ar_3–HCl cluster.[17] The constancy (or perhaps slight decrease with m) of this distance in the Ar_m–HCl system ($m = 1,2,3$) is striking. The results for Ar_m–HF are similar though not quite as dramatic.

The force constants for Ar_2–HCl from the pseudotriatomic model also seem reasonable. They are compared in Table IX with our previous results for Ar_2–H/DF. We include the stretching force constant f_R for the corresponding dimers, as determined with a pseudodiatomic model.[18] Of the force constants, f_R shows the greatest variation, ranging in the dimers from 1.17×10^{-5} dyn/Å in Ar–HCl[1] to 1.79 in Ar–DF.[3,14] For the trimers, f_R is somewhat larger (25%) but covers a smaller range (1.66–1.97). The other three force constants depend largely on the Ar_2 end of the trimer and show little variation. The Ar–Ar stretch (f_r) and torsion ($f_\beta = F_{33}/4$) are virtually independent of H/DX. The R/r stretching interaction f_{Rr} increases in proportion to f_R. The value of 0.68×10^{-5} dyn/Å found for the Ar–Ar stretch is apparently less than that for free Ar_2 for which a calculation based on the energy of the $v = 0$ and $v = 1$ levels[11] gives $f_r \sim 0.78 \times 10^{-5}$ dyn/Å.

In our work on Ar_2–H/DF the force constant for Ar_2 torsion was used to estimate the average angular displacement β. The analysis gave a value of $\sim 5°$; it depends only on f_β and I_{Ar_2} so the procedure gives the same result for Ar_2–HCl. The inertial analysis, however, gave the appreciably larger value of 7.32°, probably reflecting approximations in both estimates. Other approximations abound. For example, torsion of Ar_2 is accompanied by a displacement δb of the HCl c.m. in the ab plane, as part of ν_3, the asymmetric stretch of the pseudotriatomic complex. This adds a term $M_{HCl}\delta b^2$ to I_A and I_C and to P'_B [Eq. (6)] which can be approximated by subtracting the modified P'_B for the two chlorine isotopes. A slightly larger β results (7.33°) and a smaller r (3.856 vs 3.861 Å).

The effect of trimer formation on the Ar–Ar distance is an interesting aspect of their structure. The data available so far suggest that any such effects are modest, being comparable with the substantial uncertainties in determining r. For free Ar_2, r_0 is 3.821(10) Å. For Ar_2–HCl, -HF, and -DF, including torsional effects we have found r to be 3.861, 3.847, and 3.841 Å, respectively. This suggests trimer formation lengthens the Ar–Ar distance, but that the lengthening is less for H/DX groups which are attracted more strongly to the argon dimer. The apparent trend could be an artifact of the approximate vibrational model. However, there is a large, positive interaction (f_{Rr}) between the two stretches, which increases with f_R (Table IX).

Further studies of Ar_m–$(HX)_n$ clusters are in progress. Reports for the tetramers Ar_3–H/DF[19] and Ar_3–HCl[17] are being prepared.

ACKNOWLEDGMENTS

We thank J. M. Lisy for suggesting we try using neon first run as a carrier gas (70% Ne, 30% He). Our work was supported by a Charles W. Walton Research Grant, by the School of Chemical Sciences, and by the National Science Foundation. Acknowledgment is made to the donors of the Petroleum Research Fund, administered by the American Chemical Society, for partial support of this research.

[1] S. E. Novick, P. Davies, S. J. Harris, and W. Klemperer, J. Chem. Phys. **55**, 2273 (1973); S. E. Novick, K. C. Janda, S. L. Holmgren, M. Waldman, and W. Klemperer, *ibid.* **65**, 1114 (1976).

[2] A. C. Legon and D. J. Millen, Chem. Rev. **86**, 635 (1986).

[3] H. S. Gutowsky, T. D. Klots, C. A. Schmuttenmaer, and T. Emilsson, J. Chem. Phys. **83**, 4817 (1985); **86**, 569 (1987).

[4] H. S. Gutowsky, T. D. Klots, C. Chuang, J. D. Keen, C. A. Schmuttenmaer, and T. Emilsson, J. Am. Chem. Soc. **107**, 7174 (1985).

[5] T. J. Balle and W. H. Flygare, Rev. Sci. Instrum. **52**, 33 (1981).

[6] K. H. Bowen, Jr., Ph.D. thesis, Harvard University, 1977.

[7] E. J. Campbell, W. G. Read, and J. A. Shea, Chem. Phys. Lett. **94**, 69 (1983).

[8] H. S. Gutowsky, T. Emilsson, J. D. Keen, T. D. Klots, and C. Chuang, J. Chem. Phys. **85**, 683 (1986).

[9] W. H. Kirchhoff, J. Mol. Spectrosc. **41**, 333 (1972).

[10] J. K. G. Watson, J. Chem. Phys. **46**, 1935 (1967).

[11] E. A. Colbourn and A. E. Douglass, J. Chem. Phys. **65**, 1741 (1976).

[12] C. H. Townes and A. L. Schawlow, *Microwave Spectroscopy* (McGraw–Hill, New York, 1955), Chap. 4.

[13] F. DeLucia, P. Helminger, and W. Gordy, Phys. Rev. A **3**, 1848 (1971); E. W. Kaiser, J. Chem. Phys. **53**, 1686 (1970).

[14] M. R. Keenan, L. W. Buxton, E. J. Campbell, A. C. Legon, and W. H. Flygare, J. Chem. Phys. **74**, 2133 (1981).

[15] A. C. Legon, P. D. Aldrich, and W. H. Flygare, J. Chem. Phys. **75**, 625 (1981).

[16] W. Gordy and R. L. Cook, *Technique of Organic Chemistry* (Wiley, New York, 1970). Vol. 9, Part 2, Chap. 13.

[17] T. D. Klots, C. Chuang, R. S. Ruoff, T. Emilsson, and H. S. Gutowsky, J. Chem. Phys. (to be published).

[18] T. J. Balle, E. J. Campbell, M. R. Keenan, and W. H. Flygare, J. Chem. Phys. **71**, 2723 (1979); **72**, 922 (1980).

[19] H. S. Gutowsky, T. D. Klots, C. Chuang, J. D. Keen, C. A. Schmuttenmaer, and T. Emilsson, J. Am. Chem. Soc. (to be published).